Indoor Localization Based on Factor Graphs: A Unified Framework

Lyuxiao Yang, *Student Member, IEEE,* Nan Wu, *Member, IEEE,* Bin Li, *Member, IEEE,*
Weijie Yuan, *Member, IEEE,* and Lajos Hanzo, *Life Fellow, IEEE*

Abstract—Indoor localization is of pivotal significance for a wide variety of services in the context of the Internet of Things (IoT). Both ranging-based and fingerprint-based localization techniques are promising for employment in harsh indoor environments. Hence, we propose a unified framework based on factor graphs for ubiquitous high-accuracy indoor localization. Our unified framework efficiently integrates ranging and fingerprinting for striking an appealing accuracy versus deployment cost tradeoff, where the crowdsourcing required for the construction of fingerprinting databases can also be addressed with little human intervention. By intrinsically amalgamating the global grid sampling and the regularized importance-resampling techniques, a non-parametric belief propagation algorithm is proposed for achieving accurate position estimation at the cost of a moderate computational complexity. For improving the robustness to environmental variations, a likelihood-ratio-based approach is employed to detect ranging outliers. Moreover, a low-complexity serial scheduling scheme defined over factor graphs is designed for real-time localization. We design a hybrid UWB and Wi-Fi localization system relying on off-the-shelf commercial devices and evaluate the proposed unified framework in a typical office building. Our experimental results show that the proposed algorithm outperforms the existing state-of-the-art methods and it is capable of achieving sub-meter localization accuracy.

Index Terms—Indoor localization, unified framework, factor graph, ranging, fingerprinting.

I. INTRODUCTION

LOCATION-AWARENESS is essential for both the intelligent Internet of Things (IoT) [1] and future 6G networks [2]. Given its ever-increasing social and commercial benefits, high-accuracy indoor localization is becoming a critical factor in supporting ubiquitous location-based services (LBSs) both in the IoT and in 6G [3]–[7]. Characterized by obstacles, signal fluctuation, noise, and environmental variations, indoor environments tend to be more complex than outdoor scenarios. Yet, sub-meter-level localization accuracy is expected in advanced LBSs.

As the global navigation satellite systems (GNSSs) cannot provide reliable coverage in indoor environments [8], various alternative technologies, such as light detection and ranging (LiDAR) [9], ultrawide bandwidth (UWB) [10], Bluetooth [11], ZigBee [12] and Wi-Fi [13] aided solutions, have been investigated. For multi-antenna systems and cooperative networks, the family of angle-based localization [14], [15] and cooperative localization [16], [17] techniques have also been extensively studied. Generally, the most promising indoor localization techniques can be categorized as the ranging-based [18] and fingerprint-based [6] methods. The ranging-based schemes exploit the geometric relationships among the nodes for localization relying on time-of-arrival (TOA) [19], time-difference-of-arrival (TDOA) [20], received signal strength (RSS) [21], etc. The TOA/TDOA-based methods support high-accuracy (sub-meter-level) localization under line-of-sight (LOS) conditions, but they typically require numerous base stations (anchors). By contrast, the fingerprint-based localization (fingerprinting) techniques estimate the positions based on the similarity of wireless signal signatures, termed as fingerprints.[1] The potential fingerprints include RSS [13], channel state information (CSI) [22], etc. Fingerprinting supports ubiquitous localization based on the existing infrastructure without the need for LOS reception, at the cost of time-consuming and labor-intensive site survey for constructing fingerprinting databases. For achieving satisfactory localization accuracy at an acceptable cost, substantial research efforts have been invested [23]–[33].

For the fingerprint-based localization, the Gaussian process modeling the relationship between the fingerprints and positions in a continuous space constitutes a popular semi-supervised method of reducing the dependency on site survey [23], [24]. Crowdsourcing is another widely used technique of replacing the costly site survey by involuntary user participation [35], [36]. The LiFS technique of [25] and the GraphIPS method of [26] employ a multi-dimensional scaling algorithm, which maps distances to positions by relying on a graph-based

L. Yang, N. Wu and B. Li are with the School of Information and Electronics, Beijing Institute of Technology, Beijing 100081, China, and also with the Yangtze Delta Region Academy of Beijing Institute of Technology, Jiaxing, Zhejiang 314000, China (e-mail: bitylx@bit.edu.cn; wunan@bit.edu.cn; binli@bit.edu.cn).

W. Yuan is with the Department of Electrical and Electronic Engineering, Southern Unversity of Science and Technology, Shenzhen 518055, China (e-mail: yuanwj@sustech.edu.cn).

L. Hanzo is with the School of Electronics and Computer Science, University of Southampton, Southampton SO17 1BJ, U.K. (e-mail: lh@ecs.soton.ac.uk).

---

[1]The methods, in which the fingerprints are only used to calculate distances based on wireless signal propagation models, are classified as ranging-based ones.

TABLE I
CONTRASTING OUR UNIFIED FRAMEWORK TO THE EXISTING INDOOR LOCALIZATION SYSTEMS

	Technologies	Information sources			Crowdsourcing	Bayesian framework	Main disadvantage for practical applications	Accuracy (reported)
		Fingerprinting	Ranging	IMU				
[9]	LiDAR		✓	✓		✓	LOS only	0.1 m (small area)
[10]	UWB		✓	✓		✓	Extra anchors requirement	0.6 m
[11]	Bluetooth	✓		✓		✓	Extra anchors requirement	0.8 m
[13], [22]	Wi-Fi	✓					Costly site survey	2.1 m, 1.8 m
[34]	Wi-Fi	✓				✓	Costly site survey	0.5 m
[23], [24]	Wi-Fi	✓				✓	Costly site survey	3.9 m, 1.7 m
[25], [26]	Wi-Fi	✓		✓	✓		−	5.8 m, 1.7 m
[27]	Wi-Fi	✓			✓	✓	−	2.7 m
[28]	Wi-Fi	✓		✓	✓	✓	−	3.0 m
[12]	Wi-Fi + ZigBee	✓					Costly site survey	86% (room detection)
[29]	Wi-Fi + vision	✓	✓				Visual landmarks requirement	0.4 m
[30]	Wi-Fi + vision		✓	✓			High latency	0.2 m
[32]	Wi-Fi + UWB		✓				LOS only	0.2 m (small area)
[33]	Wi-Fi + UWB	✓	✓				1-D localization	0.1 m (narrow corridor)
Our work	**Wi-Fi + UWB**	★	★	★	✓	✓	**−**	**0.9 m**

formulation, for estimating the positions of crowdsourcing data. Within the Bayesian framework, the UCMA [27] and Zee [28] solutions harness hidden Markov models and particle filters, respectively, for constructing fingerprinting databases. Since the problem of crowdsourcing relies on a massive number of variables associated with mesh connections and different uncertainties, the above methods fail to explore all the available information therein and hence tend to suffer from performance erosion.

By intrinsically fusing multiple technologies having complementary strengths, the localization performance can be readily improved [37]. Since inertial measurement units (IMUs) are capable of providing relatively accurate walking distance estimates [38], many of the aforementioned crowdsourcing methods [25], [26], [28] harness the distance information gleaned from IMUs. Some recent contributions focus on the fusion of localization based on Wi-Fi and vision [29], [30]. Most of these contributions rely on heuristic algorithms and cannot be readily extended to different scenarios. Several papers have discussed sophisticated localization methods integrating Wi-Fi and UWB [31]–[33]. In [31], [32], Wi-Fi RSS readings are employed for merely ranging instead of fingerprinting, neglecting the fingerprint-induced proximity information. Although the scheme of [33] has integrated fingerprinting and ranging to a certain extent, it is heuristic and only suitable for narrow corridors (1-D localization). To substantially improve the accuracy vs. cost trade-off in indoor localization, developing a unified framework for efficiently fusing multi-source information is quite challenging.

Motivated by tackling this challenge, we represent the indoor localization problem by a factor graph [39] and provide a unified treatment of ranging and fingerprinting. The proposed method is implemented and evaluated in a hybrid localization system based on UWB and Wi-Fi for demonstrating their potentials in practical deployment. For multi-source fusion localization based on ranging, factor graphs have already been shown to constitute a powerful framework [40]–[44]. To incorporate data-driven fingerprinting into this framework, we employ the so-called log-distance path loss (LDPL) model of [45], and develop a position proximity model. In this way, we are able to integrate fingerprinting as well as ranging, and address diverse scenarios, including crowdsourcing and real-time localization based on a unified framework. Since environmental variations may lead to large measurement errors [46], we develop a likelihood-ratio-based outlier detector. To reduce the computation time of real-time localization, we also design a scheduling scheme based on factor graphs. Since the uncertainties of the various measurements collected are carefully considered, our method is capable of efficiently fusing the multi-source position information, hence improving the localization accuracy attained. The features of the proposed unified framework are boldly and explicitly contrasted to the literature in Table I. For the information sources in Table I, ✓ indicates that this information is necessary for the system to work, while ★ indicates that the scheme is indeed capable of exploiting this information, but it can also operate without it.

The main contributions of this paper are summarized as follows:

- We propose a unified framework for indoor localization constructed over factor graphs, which facilitates the fu-

sion of ranging-based and fingerprint-based localization relying on crowdsourcing. The data-driven fingerprinting are integrated into the framework in the form of factor nodes based on a position proximity model, which is built by employing the Gaussian kernel and the K-nearest neighbor (KNN) algorithm.

- In order to achieve high-accuracy localization, we develop a non-parametric belief propagation (BP) algorithm based on factor graphs by intrinsically combining the grid sampling [47] and the regularized importance-resampling [48] techniques for tackling the problem of having local optima and the loss of sufficiently rich sample diversity, despite reducing the complexity. A ranging outlier detection method based on the likelihood ratio is also proposed for improving the robustness to the environmental variations. Furthermore, we design a low-complexity scheduling scheme constructed over factor graphs for meeting the low latency requirement of real-time localization at a negligible performance erosion.

- We develop a hybrid localization prototype based on UWB as well as Wi-Fi, and conduct extensive experiments in a typical office building for evaluating the proposed method. The experimental results show that our method achieves excellent localization performance compared to the state-of-the-art methods. The average error of crowdsourcing is 1.7 m for the Wi-Fi-based system and 0.9 m for the hybrid system. For real-time localization scenarios, the average error becomes 1.8 m and 0.9 m, respectively.

The remainder of this paper is organized as follows. The system model is introduced in Section II. In Section III, our unified factor graph framework is established and the position estimation algorithm is developed for addressing the challenges of indoor localization. Section IV presents our experimental setup and discusses our results. Finally, our conclusions are offered in Section V.

Notations: Italic and lower-case boldface letters represent scalars and vectors, respectively; Upper-case calligraphic letters (e.g., $\mathcal{X}$) denote sets; In particular, $\mathcal{I}$ denotes the index set. $\|\cdot\|$ denotes the Euclidean norm; $\delta\left(\cdot\right)$ denotes the Dirac delta function; $\mathcal{U}\left(a, b\right)$ represents a uniform distribution with lower bound a and upper bound b; The operation $\lceil\cdot\rceil$ returns the nearest integer greater than or equal to the element. Additionally, the acronyms are listed in Table II.

II. SYSTEM MODEL

In indoor localization scenarios, the position-related information is contained in the floor plan, user observations, and landmarks. For the typical UWB and Wi-Fi hybrid localization system of Fig. 1, the user observations include the UWB ranging, Wi-Fi RSS, and IMU readings. In order to establish a unified indoor localization algorithm framework, we construct probabilistic models for representing the various position-related information.

A. Floor Plan

The floor plan of a region of interest can be modeled as the *a priori* distribution of the i-th user's position $\mathbf{x}_i$ for localization.

TABLE II
LIST OF ACRONYMS

| Acronym	Definition
AP	Access point
BP	Belief propagation
CDF	Cumulative distribution function
CSI	Channel state information
FN	Factor node
GNSS	Global navigation satellite system
GT	Ground-truth
IMU	Inertial measurement unit
IoT	Internet of Things
KNN	K-nearest neighbor
LBS	Location-based service
LDPL	Log-distance path loss
LiDAR	Light detection and ranging
LOS	Line-of-sight
MAE	Mean absolute error
MAP	Maximum *a posteriori*
MaxE	Maximum error
MMSE	Minimum mean square error
NLOS	Non-line-of-sight
NN	Nearest neighbor
OD	Outlier detection
PI	Proximity information
RMSE	Root mean square error
RSS	Received signal strength
TDOA	Time-difference-of-arrival
TOA	Time-of-arrival
TSML	Two-stage maximum-likelihood
UWB	Ultrawide bandwidth
VN	Variable node
WKNN	Weighted K-nearest neighbor
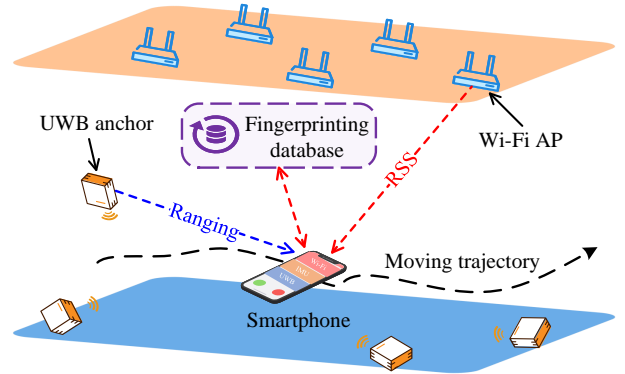
Fig. 1. Illustration of UWB and Wi-Fi hybrid localization system.

In the absence of any *a priori* knowledge, such as the user's behavior, a natural choice for the probabilistic model of a floor plan is a uniform distribution formulated as:

$$p_{\mathrm{map}}\left(\mathbf{x}_i\right) \propto \begin{cases} 1, & \mathbf{x}_i \in \mathcal{A} \\ 0, & \text{otherwise} \end{cases}, \qquad (1)$$

where $\mathcal{A}$ denotes the region that the users can reach.

B. UWB Ranging

When the positions of certain UWB access points (APs), termed as UWB anchors, are known, they can provide valuable

position information in the form of ranging. Let us assume that there are N_{u} UWB anchors having the positions of $\mathcal{X}^{\mathrm{u}} = \{\mathbf{x}_k^{\mathrm{u}}, k \in \mathcal{I}^{\mathrm{u}}\}$, where $\mathcal{I}^{\mathrm{u}}$ denotes the index set of all the UWB anchors. The UWB ranging measurements of the i-th user are $\mathbf{d}_i^{\mathrm{u}} = \left[d_{i,k}^{\mathrm{u}}, k \in \mathcal{I}_i^{\mathrm{u}} \right]$, where $\mathcal{I}_i^{\mathrm{u}} \subseteq \mathcal{I}^{\mathrm{u}}$ refers to the index set of the UWB anchors within the communication range of $\mathbf{x}_i$, and

$$d_{i,k}^{\mathrm{u}} = \|\mathbf{x}_i - \mathbf{x}_k^{\mathrm{u}}\| + b^{\mathrm{u}} + \omega^{\mathrm{u}}, \tag{2}$$

where b^{u} is the bias caused by non-line-of-sight (NLOS) propagation which is generally Rayleigh distributed, and ω^{u} is the Gaussian measurement inaccuracy [19].

If $\mathbf{x}_i$ and $\mathbf{x}_k^{\mathrm{u}}$ are in LOS condition, b^{u} is zero. According to (2), we have

$$p_{\mathrm{uwb}}\left(d_{i,k}^{\mathrm{u}}|\mathbf{x}_i, \mathbf{x}_k^{\mathrm{u}}\right) = \frac{1}{\sqrt{2\pi}\sigma_{\mathrm{u}}} \exp\left[-\frac{\left(\|\mathbf{x}_i - \mathbf{x}_k^{\mathrm{u}}\| - d_{i,k}^{\mathrm{u}}\right)^2}{2\sigma_{\mathrm{u}}^2} \right],$$
$$\tag{3}$$

where σ_{u}^2 is the variance of the measurement noise. If $\mathbf{x}_i$ and $\mathbf{x}_k^{\mathrm{u}}$ are in NLOS condition, b^{u} dominates the measurement error [49]. Accordingly, ω^{u} can be ignored and the likelihood function is rewritten as

$$p_{\mathrm{uwb}}\left(d_{i,k}^{\mathrm{u}}|\mathbf{x}_i, \mathbf{x}_k^{\mathrm{u}}\right) = \frac{\left(d_{i,k}^{\mathrm{u}} - \|\mathbf{x}_i - \mathbf{x}_k^{\mathrm{u}}\|\right)}{\xi_{\mathrm{u}}^2}$$
$$\times \exp\left[-\frac{\left(d_{i,k}^{\mathrm{u}} - \|\mathbf{x}_i - \mathbf{x}_k^{\mathrm{u}}\|\right)^2}{2\xi_{\mathrm{u}}^2} \right],$$
$$d_{i,k}^{\mathrm{u}} - \|\mathbf{x}_i - \mathbf{x}_k^{\mathrm{u}}\| \geq 0, \tag{4}$$

where ξ_{u} is the parameter of the Rayleigh distribution.

C. Wi-Fi RSS

Let us assume that N_{w} Wi-Fi APs can be detected in the building. Furthermore, $\mathbf{r}_i = [r_{i,1}, r_{i,2}, \cdots, r_{i,N_{\mathrm{w}}}]$ represent the Wi-Fi RSS vector (Wi-Fi fingerprint) of the i-th user. When the positions of some Wi-Fi APs are known, which are denoted by $\mathcal{X}^{\mathrm{w}} = \{\mathbf{x}_k^{\mathrm{w}}, k \in \mathcal{I}^{\mathrm{w}}\}$, they can provide position information by means of wireless propagation models. According to the LDPL model,

$$r_{i,k} = \beta - 10\gamma \lg\left(\frac{\|\mathbf{x}_i - \mathbf{x}_k^{\mathrm{w}}\|}{d_0} \right) + \omega^{\mathrm{ldpl}}, \tag{5}$$

where β is a constant, γ is the path loss exponent, d_0 is the reference distance, and ω^{ldpl} is a Gaussian random variable. The values of β and γ mainly depend on the propagation environment, e.g., LOS and NLOS [27]. According to (5), the likelihood function is given by

$$p_{\mathrm{ldpl}}\left(r_{i,k}|\mathbf{x}_i, \mathbf{x}_k^{\mathrm{w}}\right) =$$
$$\frac{1}{\sqrt{2\pi}\sigma_{\mathrm{ldpl}}} \exp\left\{ -\frac{[\beta - 10\gamma \lg(\|\mathbf{x}_i - \mathbf{x}_k^{\mathrm{w}}\|/d_0) - r_{i,k}]^2}{2\sigma_{\mathrm{ldpl}}^2} \right\},$$
$$\tag{6}$$

where σ_{ldpl}^2 is the variance of ω^{ldpl}.

Existing studies have shown that the distributions of the positions associated to similar Wi-Fi fingerprints have obvious correlation [34], [50]–[53], while the Gaussian kernels have been widely used to depict the relationship between fingerprints and positions [23], [24], [34]. Inspired by this, we propose a position proximity model based on the similarity of Wi-Fi fingerprints and the Gaussian functions. The methods of finding similar fingerprints include threshold-based processing [25], clustering [54], [55], KNN classifiers [13], etc, where the KNN algorithm strikes the best performance vs. complexity trade-off. For the fingerprint $\mathbf{r}_i$, we find K nearest neighbors based on the Euclidean distances. Upon considering similar fingerprints, the probability that a pair of fingerprints are from the same position is inversely proportional to their Euclidean distance [51]–[53]. According to this principle, if the k-th nearest neighbor of $\mathbf{r}_i$ is $\mathbf{r}_j$, we assume that

$$p_{\mathrm{nn}}\left(\mathbf{r}_i, \mathbf{r}_j|\mathbf{x}_i, \mathbf{x}_j\right) = \frac{1}{\sqrt{2\pi}\sigma_{\mathrm{nn},k}} \exp\left(-\frac{\|\mathbf{x}_i - \mathbf{x}_j\|^2}{2\sigma_{\mathrm{nn},k}^2} \right), \tag{7}$$

where $\sigma_{\mathrm{nn},k} = \sigma_{\mathrm{nn}} \|\mathbf{r}_i - \mathbf{r}_j\| / \|\mathbf{r}_i - \mathbf{r}_l\|$ increasing with the increase of $\|\mathbf{r}_i - \mathbf{r}_j\|$, $\mathbf{r}_l$ is the nearest neighbor of $\mathbf{r}_i$, and σ_{nn} is a constant corresponding to the root mean square error (RMSE) of the fingerprinting based on the nearest neighbor (NN) algorithm.

D. Inertial Measurement Unit

By processing the data gleaned from IMUs, especially accelerometer sensors, we can obtain the walking distance measurements of adjacent observations [25]. The walking distance measurement between $\mathbf{x}_i$ and $\mathbf{x}_{i+1}$ is given by

$$d_{i,i+1}^{\mathrm{imu}} = \|\mathbf{x}_i - \mathbf{x}_{i+1}\| + \omega^{\mathrm{imu}}, \tag{8}$$

where the measurement error ω^{imu} is assumed to be Gaussian distributed [28], [56]. Accordingly, we have

$$p_{\mathrm{imu}}\left(d_{i,i+1}^{\mathrm{imu}}|\mathbf{x}_i, \mathbf{x}_{i+1}\right) = \frac{1}{\sqrt{2\pi}\sigma_{\mathrm{imu}}}$$
$$\times \exp\left[-\frac{\left(\|\mathbf{x}_i - \mathbf{x}_{i+1}\| - d_{i,i+1}^{\mathrm{imu}}\right)^2}{2\sigma_{\mathrm{imu}}^2} \right],$$
$$\tag{9}$$

where σ_{imu}^2 is the variance of ω^{imu}.

E. Landmarks

The *a priori* distribution of the position of a landmark can be expressed as

$$p_{\mathrm{lm}}\left(\mathbf{x}\right) \propto \delta\left(\mathbf{x} - \tilde{\mathbf{x}}\right), \tag{10}$$

where $\tilde{\mathbf{x}}$ denotes the ground-truth or estimated value of $\mathbf{x}$. In addition to the UWB anchors and the Wi-Fi APs that can be regarded as landmarks, we mainly consider the Wi-Fi landmarks having the positions of $\mathcal{X}^{\mathrm{wlm}} = \{\mathbf{x}_j^{\mathrm{wlm}}, j \in \mathcal{I}^{\mathrm{wlm}}\}$ and the Wi-Fi fingerprints of $\mathcal{R}^{\mathrm{wlm}} = \{\mathbf{r}_j^{\mathrm{wlm}}, j \in \mathcal{I}^{\mathrm{wlm}}\}$, which provide certain position information by combining the position proximity model described in Section II-C. The Wi-Fi landmarks can be obtained through site survey, or accurate position estimation from the historical data collected by users.

III. A Unified Framework for Indoor Localization Based on Factor Graphs

Given the floor plan, the landmarks and N user observations $\mathcal{O} = \{\mathcal{O}_1, \mathcal{O}_2, \cdots, \mathcal{O}_N\}$, the goal is to estimate the corresponding positions $\mathcal{X} = \{\mathbf{x}_1, \mathbf{x}_2, \cdots, \mathbf{x}_N\}$, where $\mathbf{x}_i \triangleq [x_i, y_i]^{\mathrm{T}}$ and $\mathcal{O}_i \triangleq \{\mathbf{d}_i^{\mathrm{u}}, \mathbf{r}_i, d_{i,i-1}^{\mathrm{imu}}\}$. For convenience, $\mathcal{I}^{\mathcal{X}}$ represents the index set of all the variables in $\mathcal{X}$, $\mathcal{R} = \{\mathbf{r}_i, i \in \mathcal{I}^{\mathcal{X}}\}$, and $\mathcal{X}^{\mathrm{a}} = \mathcal{X} \cup \mathcal{X}^{\mathrm{wlm}} \cup \mathcal{X}^{\mathrm{u}} \cup \mathcal{X}^{\mathrm{w}}$. In the following, we propose a unified framework for indoor localization based on factor graphs.

A. Factor Graph Representation

From the perspective of Bayesian inference, we can obtain the minimum mean square error (MMSE) or maximum *a posteriori* (MAP) estimate of $\mathbf{x}_i$ based on the marginal *a posteriori* distribution

$$p(\mathbf{x}_i | \mathcal{O}) = \int p(\mathcal{X}^{\mathrm{a}} | \mathcal{O}) \, \mathrm{d}\mathcal{X}^{\mathrm{a}} \backslash \mathbf{x}_i, \tag{11}$$

where $p(\mathcal{X}^{\mathrm{a}} | \mathcal{O})$ is the joint *a posteriori* distribution of all the positions. Integrating such a large number of variables is generally intractable. Nonetheless, we succeeded in carrying out this factorization to construct the factor graph and exploit the message passing algorithm for efficiently calculating (11).

The specific pattern of factorization directly affects the efficiency of the algorithm. To establish the sufficient and necessary factors, considering the physical meaning, we factorize the joint *a posteriori* distribution according to the position-related information gleaned from five sources as shown in Section II. According to Bayes' theorem, we have

$$p(\mathcal{X}^{\mathrm{a}} | \mathcal{O}) \propto p(\mathcal{O} | \mathcal{X}^{\mathrm{a}}) p(\mathcal{X}^{\mathrm{a}}). \tag{12}$$

where $p(\mathcal{X}^{\mathrm{a}})$ denotes the joint *a priori* distribution, and $p(\mathcal{O} | \mathcal{X}^{\mathrm{a}})$ is the global likelihood function. The floor plan and the landmarks provide the *a priori* information for localization. Therefore, $p(\mathcal{X}^{\mathrm{a}})$ can be factorized as

$$p(\mathcal{X}^{\mathrm{a}}) \propto \prod_{i=1}^{N} p_{\mathrm{map}}(\mathbf{x}_i) \prod_{k \in \mathcal{I}^{\mathrm{u}}} p_{\mathrm{lm}}(\mathbf{x}_k^{\mathrm{u}}) \prod_{k \in \mathcal{I}^{\mathrm{w}}} p_{\mathrm{lm}}(\mathbf{x}_k^{\mathrm{w}}) \prod_{j \in \mathcal{I}^{\mathrm{wlm}}} p_{\mathrm{lm}}(\mathbf{x}_j^{\mathrm{wlm}}). \tag{13}$$

Since the measurements from the UWB, Wi-Fi and IMU modules as well as from each observation are independent, the global likelihood function can be written as

$$p(\mathcal{O} | \mathcal{X}^{\mathrm{a}}) \propto \prod_{i=1}^{N} \left[\prod_{k \in \mathcal{I}_i^{\mathrm{u}}} p_{\mathrm{uwb}}\left(d_{i,k}^{\mathrm{u}} | \mathbf{x}_i, \mathbf{x}_k^{\mathrm{u}}\right) \right.$$
$$\times \prod_{k \in \mathcal{I}^{\mathrm{w}}} p_{\mathrm{ldpl}}\left(r_{i,k} | \mathbf{x}_i, \mathbf{x}_k^{\mathrm{w}}\right) \prod_{j \in \mathcal{I}_i^{\mathcal{N}_1}} p_{\mathrm{nn}}\left(\mathbf{r}_i, \mathbf{r}_j^{\mathrm{wlm}} | \mathbf{x}_i, \mathbf{x}_j^{\mathrm{wlm}}\right)$$
$$\left. \times \prod_{j \in \mathcal{I}_i^{\mathcal{N}_2}} p_{\mathrm{nn}}\left(\mathbf{r}_i, \mathbf{r}_j | \mathbf{x}_i, \mathbf{x}_j\right) \prod_{j \in \mathcal{I}_i^{\mathcal{T}}} p_{\mathrm{imu}}\left(d_{i,j}^{\mathrm{imu}} | \mathbf{x}_i, \mathbf{x}_j\right) \right], \tag{14}$$

where $\mathcal{I}_i^{\mathcal{N}_1} \subset \mathcal{I}^{\mathrm{wlm}}$ and $\mathcal{I}_i^{\mathcal{N}_2} \subset \mathcal{I}^{\mathcal{X}}$ denote the index sets of the neighbors of $\mathbf{r}_i$ in $\mathcal{R}^{\mathrm{wlm}}$ and $\mathcal{R}$ respectively, while $\mathcal{I}_i^{\mathcal{T}} \subset \mathcal{I}^{\mathcal{X}}$ denotes the index set of the adjacent observations of $\mathbf{o}_i$.
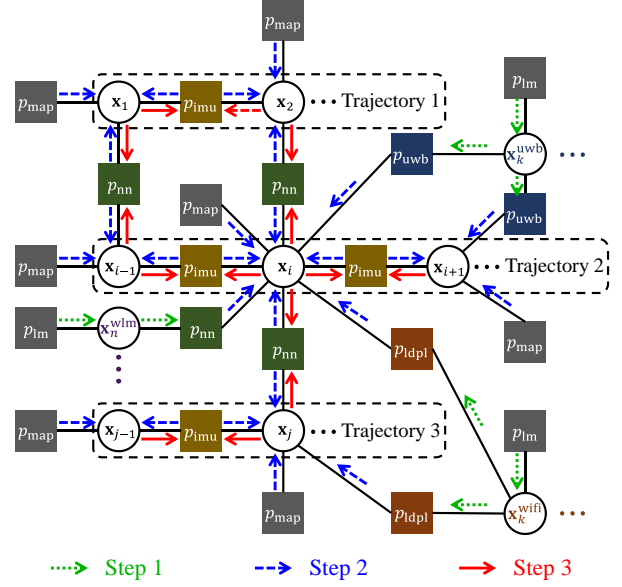

Fig. 2. Factor graph of indoor localization in UWB and Wi-Fi hybrid system and illustration of message passing scheduling.

A factor graph is a bipartite graph representing the dependence between variables and factors. In this paper, we use a circle to represent a variable node (VN), which corresponds to the position of a user, and use a rectangle to represent a factor node (FN), which corresponds to an *a priori* or likelihood function. According to the aforementioned factorization pattern, we can obtain a factor graph of indoor localization, as shown in Fig. 2, where a FN is connected to a VN, if and only if this factor is a function of this variable. By passing messages between VNs and FNs, we can obtain the approximate marginal distribution of the positions. In this way, we are capable of fusing multi-source heterogeneous information for localization based on the proposed unified factor graph framework.

B. Position Estimation Based on Belief Propagation

To solve the position estimation problem represented by a factor graph, we employ BP for finding the approximate marginal distributions, a.k.a., beliefs.

Due to the mutual relationships between variables, the factor graph of indoor localization is a loopy one, on which the BP performs the following two steps iteratively:

(i) For each FN g, the outgoing message passed to its connected VNs is calculated by

$$\mu_{g \to i}^{\mathrm{f}}(\mathbf{x}_i) \propto \int p\left(\mathbf{x}_{\mathcal{I}_g^{\mathrm{f}}}\right) \prod_{j \in \mathcal{I}_g^{\mathrm{f}} \backslash i} \mu_{j \to g}^{\mathrm{v}}(\mathbf{x}_j) \, \mathrm{d}\mathbf{x}_{\mathcal{I}_g^{\mathrm{f}} \backslash i}, \tag{15}$$

where $\mathcal{I}_g^{\mathrm{f}}$ refers to the index set of the VNs connected to the FN g, and $p(\mathbf{x}_{\mathcal{I}})$ denotes the function of the variables $\mathbf{x}_k, k \in \mathcal{I}$.

(ii) For each VN i, the outgoing message passed to its connected FNs is calculated by

$$\mu_{i\to g}^{\mathrm{v}}\left(\mathbf{x}_i\right) \propto \prod_{h\in\mathcal{I}_i^{\mathrm{v}}\setminus g} \mu_{h\to i}^{\mathrm{f}}\left(\mathbf{x}_i\right), \qquad (16)$$

where $\mathcal{I}_i^{\mathrm{v}}$ refers to the index set of the FNs connected to the VN i.

After a few iterations, the belief of the variable $\mathbf{x}_i$ is computed as

$$b\left(\mathbf{x}_i\right) \propto \prod_{h\in\mathcal{I}_i^{\mathrm{v}}} \mu_{h\to i}^{\mathrm{f}}\left(\mathbf{x}_i\right). \qquad (17)$$

To reduce the computational complexity, we approximate the messages $\mu_{i\to g}^{\mathrm{v}}\left(\mathbf{x}_i\right), g\in\mathcal{I}_i^{\mathrm{v}}$ in (16) by $b\left(\mathbf{x}_i\right)$ as in [40].

Due to the non-Gaussian terms involved in the factorization in (14), it is intractable to determine closed-form expressions for the messages. To this end, we propose a non-parametric sample-based BP for indoor localization, where the beliefs in (17) are represented by samples.

Assume that at the t-th iteration, the belief of $\mathbf{x}_i$ is depicted by the samples $\mathcal{X}_{\mathrm{b}}^{(t)} = \left\{\dot{\mathbf{x}}_{i,n}^{(t)}, n=1,2,\cdots,N_{\mathrm{b}}\right\}$ having equal weight.[2] The beliefs are updated in the style of importance-resampling at each iteration. Additionally, we embed the global grid sampling into the importance-resampling process for avoiding local optima. Specifically, $\mathcal{X}_{\mathrm{b}}^{(t)}$ are drawn from not only $\mathcal{X}_{\mathrm{b}}^{(t-1)}$ but also from a set of auxiliary grid samples $\mathcal{X}_{\mathrm{g}}$, which are drawn from $\mathcal{A}$ associated with a fixed grid size l_{g}. For convenience, we define $\mathcal{X}_{\mathrm{s}}^{(t-1)} = \mathcal{X}_{\mathrm{b}}^{(t-1)} \cup \mathcal{X}_{\mathrm{g}}$ and $N_{\mathrm{s}}^{(t)}$ as the number of elements in $\mathcal{X}_{\mathrm{s}}^{(t)}$, where $\mathcal{X}_{\mathrm{s}}^{(t-1)}$ are the samples of the proposal distribution at the t-th iteration.[3]

To update the samples $\mathcal{X}_{\mathrm{b}}$ via BP, the importance weights of samples of the proposal distribution are calculated according to (15) and (17). Specifically, at the t-th iteration, the weight of the n-th sample is expressed as

$$w_{i,n}^{(t-1)} \propto \prod_{g\in\mathcal{I}_i^{\mathrm{v}}} \mu_{g\to i}^{\mathrm{f}}\left(\dot{\mathbf{x}}_{i,n}^{(t-1)}\right). \qquad (19)$$

There are two types of factors in (19), i.e. the *a priori* and the likelihood factors. The message passed from the *a priori* FN g to $\mathbf{x}_i$ is formulated by

$$\mu_{g\to i}^{\mathrm{f_{pri}}}\left(\dot{\mathbf{x}}_{i,n}^{(t-1)}\right) \propto p\left(\dot{\mathbf{x}}_{i,n}^{(t-1)}\right). \qquad (20)$$

where $p\left(\mathbf{x}_i\right)$ is the function $p_{\mathrm{map}}\left(\mathbf{x}_i\right)$ in (1), or $p_{\mathrm{lm}}\left(\mathbf{x}_i\right)$ in (10). The message passed from the likelihood FN g to $\mathbf{x}_i$ is represented by

$$\mu_{g\to i}^{\mathrm{f_{lik}}}\left(\dot{\mathbf{x}}_{i,n}^{(t-1)}\right) \propto \int p\left(\dot{\mathbf{x}}_{i,n}^{(t-1)}, \mathbf{x}_j\right) \dot{b}^{(t-1)}\left(\mathbf{x}_j\right)\mathrm{d}\mathbf{x}_j. \qquad (21)$$

If $\mathbf{x}_j$ corresponds to a landmark, according to (10), we have

$$\mu_{g\to i}^{\mathrm{f_{lik}}}\left(\dot{\mathbf{x}}_{i,n}^{(t-1)}\right) \propto p\left(\dot{\mathbf{x}}_{i,n}^{(t-1)}, \tilde{\mathbf{x}}_j\right), \qquad (22)$$

[2]The discrete approximate belief of $\mathbf{x}_i$ is expressed as

$$\dot{b}^{(t)}\left(\mathbf{x}_i\right) = \frac{1}{N_{\mathrm{b}}} \sum_{n=1}^{N_{\mathrm{b}}} \delta\left(\mathbf{x}_i - \dot{\mathbf{x}}_{i,n}^{(t)}\right). \qquad (18)$$

[3]Let $\mathcal{X}_{\mathrm{s}}^{(-1)} = \mathcal{X}_{\mathrm{g}}$ for initialization.

where $p\left(\mathbf{x}_i, \mathbf{x}_j\right)$ is the function $p_{\mathrm{uwb}}\left(d_{i,j}^{\mathrm{u}}|\mathbf{x}_i, \mathbf{x}_j\right)$ in (3) or (4), $p_{\mathrm{ldpl}}\left(r_{i,j}|\mathbf{x}_i, \mathbf{x}_j\right)$ in (6), or $p_{\mathrm{nn}}\left(\mathbf{r}_i, \mathbf{r}_j|\mathbf{x}_i, \mathbf{x}_j\right)$ in (7). Since the model of UWB ranging and the parameters of the LDPL model are different for LOS and NLOS conditions, we have to partition $\left\{\dot{\mathbf{x}}_{i,n}^{(t-1)}\right\}$ into the positions in LOS and NLOS for each UWB anchor and Wi-Fi AP by referring to the floor plan. If $\mathbf{x}_j$ corresponds to an observation, upon substituting (18) into (21), we obtain

$$\mu_{g\to i}^{\mathrm{f_{lik}}}\left(\dot{\mathbf{x}}_{i,n}^{(t-1)}\right) \propto \sum_{m=1}^{N_{\mathrm{b}}} p\left(\dot{\mathbf{x}}_{i,n}^{(t-1)}, \dot{\mathbf{x}}_{j,m}^{(t-1)}\right), \qquad (23)$$

where $p\left(\mathbf{x}_i, \mathbf{x}_j\right)$ is the function $p_{\mathrm{nn}}\left(\mathbf{r}_i, \mathbf{r}_j|\mathbf{x}_i, \mathbf{x}_j\right)$ in (7) or $p_{\mathrm{imu}}\left(d_{i,j}^{\mathrm{imu}}|\mathbf{x}_i, \mathbf{x}_j\right)$ in (9). Furthermore, we normalize the weights by

$$\dot{w}_{i,n}^{(t-1)} = \frac{w_{i,n}^{(t-1)}}{\sum_{m=1}^{N_{\mathrm{s}}^{(t-1)}} w_{i,m}^{(t-1)}}. \qquad (24)$$

Moreover, based on the normalized weights, we employ the regularized importance-resampling [48] to draw the samples $\mathcal{X}_{\mathrm{b}}^{(t)}$ from a continuous function rather than a discrete one, which can avoid the problem of insufficient sample diversity.

For accurately estimating the beliefs of all the variables, we harness the so-called flooding scheduling [57] on the loopy factor graph in Fig. 2, which is summarized as follows:

Step 1: Calculate the messages from landmark-related *a priori* FNs to likelihood FNs according to (20) and (19) sequentially, which are represented by the green dotted arrows, for initialization.

Step 2: Calculate the messages from FNs to VNs according to (20), (22) or (23) in parallel, which are represented by the blue dashed arrows.

Step 3: Calculate the messages from VNs to observation-related likelihood FNs (beliefs) according to (19) in parallel, which are represented by the red solid arrows.

Step 4: Repeat step 2 and step 3 until reaching the terminated conditions.

Based on the resultant beliefs, we estimate the i-th observation's position according to the MMSE criterion as

$$\hat{\mathbf{x}}_i = \frac{1}{N_{\mathrm{b}}} \sum_{n=1}^{N_{\mathrm{b}}} \dot{\mathbf{x}}_{i,n}^{(t)}, \; i\in\mathcal{I}^{\mathcal{X}}. \qquad (25)$$

Our non-parametric BP algorithm proposed for indoor localization is summarized in **Algorithm 1**.

C. Outlier Detection

Due to the environmental variations, ranging outliers may occur, which have to be detected and eliminated for maintaining high localization accuracy. If $d_{i,k}^{\mathrm{u}}$ is an outlier, we have $d_{i,k}^{\mathrm{u}} = \omega^{\mathrm{uo}}$, where $\omega^{\mathrm{uo}} \sim \mathcal{U}\left(0, d_{\max}^{\mathrm{u}}\right)$. By introducing a binary variable $\kappa_{i,k}^{\mathrm{u}}$, (2) can be rewritten as

$$d_{i,k}^{\mathrm{u}} = \left(1 - \kappa_{i,k}^{\mathrm{u}}\right)\left(\|\mathbf{x}_i - \mathbf{x}_k^{\mathrm{u}}\| + b^{\mathrm{u}} + \omega^{\mathrm{u}}\right) + \kappa_{i,k}^{\mathrm{u}}\omega^{\mathrm{uo}}, \qquad (26)$$

where $\kappa_{i,k}^{\mathrm{u}} = 1$ indicates that $d_{i,k}^{\mathrm{u}}$ is an outlier and vice versa. Under the assumption that the occurrence probability

Algorithm 1 Non-Parametric BP for Indoor Localization

Input: floorplan $\mathcal{A}$, landmarks $\mathcal{X}^{\mathrm{u}}$, $\mathcal{X}^{\mathrm{w}}$, $\left\{ \mathcal{X}^{\mathrm{wlm}}, \mathcal{R}^{\mathrm{wlm}} \right\}$, and user observations $\mathcal{O}$,

Output: postions $\{\hat{\mathbf{x}}_i\}$

1: Draw the grid samples $\mathcal{X}_{\mathrm{g}}$ in $\mathcal{A}$ with the grid size l_{g}
2: Initialize $\mathcal{X}_{\mathrm{s}}^{(-1)} = \mathcal{X}_{\mathrm{g}}, t = 0$
3: **repeat**
4:    **for** $i = 1$ to N **do**
5:       **for** $n = 1$ to $N_{\mathrm{s}}^{(t)}$ **do**
6:          Calculate the normalized weight $\dot{w}_{i,n}^{(t-1)}$ according to (24) and (19) based on the scheduling
7:       **end for**
8:    Draw the belief samples $\mathcal{X}_{\mathrm{b}}^{(t)}$ from $\mathcal{X}_{\mathrm{s}}^{(t-1)}$ by using the regularized importance-resampling
9:    **end for**
10:   $t = t + 1$
11: **until** reaching the terminated conditions
12: **for** $i = 1$ to N **do**
13:   Calculate $\hat{\mathbf{x}}_i$ according to (25)
14: **end for**

Fig. 3. Illustration of low-complexity scheduling for real-time localization.

of outliers is p_{o}, the *a priori* distribution of $\kappa_{i,k}^{\mathrm{u}}$ is governed by the Bernoulli distribution [58]:

$$p\left(\kappa_{i,k}^{\mathrm{u}}\right) = p_{\mathrm{o}}^{\kappa_{i,k}^{\mathrm{u}}} \left(1 - p_{\mathrm{o}}\right)^{1 - \kappa_{i,k}^{\mathrm{u}}}. \tag{27}$$

In **Algorithm 1**, we estimate the state of $\kappa_{i,k}^{\mathrm{u}}$ at the end of each iteration based on the likelihood ratio of

$$\begin{aligned}
\lambda\left(d_{i,k}^{\mathrm{u}}\right) &= \frac{p\left(d_{i,k}^{\mathrm{u}}, \mathbf{x}_i, \mathbf{x}_k^{\mathrm{u}} | \kappa_{i,k}^{\mathrm{u}} = 1\right) p\left(\kappa_{i,k}^{\mathrm{u}} = 1\right)}{p\left(d_{i,k}^{\mathrm{u}}, \mathbf{x}_i, \mathbf{x}_k^{\mathrm{u}} | \kappa_{i,k}^{\mathrm{u}} = 0\right) p\left(\kappa_{i,k}^{\mathrm{u}} = 0\right)} \\
&= \frac{p\left(d_{i,k}^{\mathrm{u}}, \mathbf{x}_i, \mathbf{x}_k^{\mathrm{u}} | \kappa_{i,k}^{\mathrm{u}} = 1\right) p_{\mathrm{o}}}{p\left(d_{i,k}^{\mathrm{u}}, \mathbf{x}_i, \mathbf{x}_k^{\mathrm{u}} | \kappa_{i,k}^{\mathrm{u}} = 0\right) \left(1 - p_{\mathrm{o}}\right)}
\end{aligned} \tag{28}$$

for all observed $d_{i,k}^{\mathrm{u}}$. According to (26), we know that $p\left(d_{i,k}^{\mathrm{u}}, \mathbf{x}_i, \mathbf{x}_k^{\mathrm{u}} | \kappa_{i,k}^{\mathrm{u}} = 1\right) = 1/d_{\max}^{\mathrm{u}}$. Based on the message passing rules of BP and the sample representation in (18), at the t-th iteration, we have

$$p\left(d_{i,k}^{\mathrm{u}}, \mathbf{x}_i, \mathbf{x}_k^{\mathrm{u}} | \kappa_{i,k}^{\mathrm{u}} = 0\right) = \frac{1}{N_{\mathrm{b}}} \sum_{n=1}^{N_{\mathrm{b}}} p_{\mathrm{uwb}}\left(d_{i,k}^{\mathrm{u}} | \dot{\mathbf{x}}_{i,n}^{(t)}, \mathbf{x}_k^{\mathrm{u}}\right). \tag{29}$$

If $\lambda\left(d_{i,k}^{\mathrm{u}}\right) > 1$, $d_{i,k}^{\mathrm{u}}$ is regarded as an outlier, and the factor containing $d_{i,k}^{\mathrm{u}}$ will be discarded at the next iteration of message passing.

D. Real-Time Localization

The above flooding scheduling estimates the positions of all the observations, thus leading to high computational complexity, which is more applicable to crowdsourcing. To meet the low latency requirement of real-time localization, we propose a low-complexity serial scheduling scheme dispensing with any iterative processing. Specifically, in real-time localization, we only update the messages gleaned from the nodes connected to
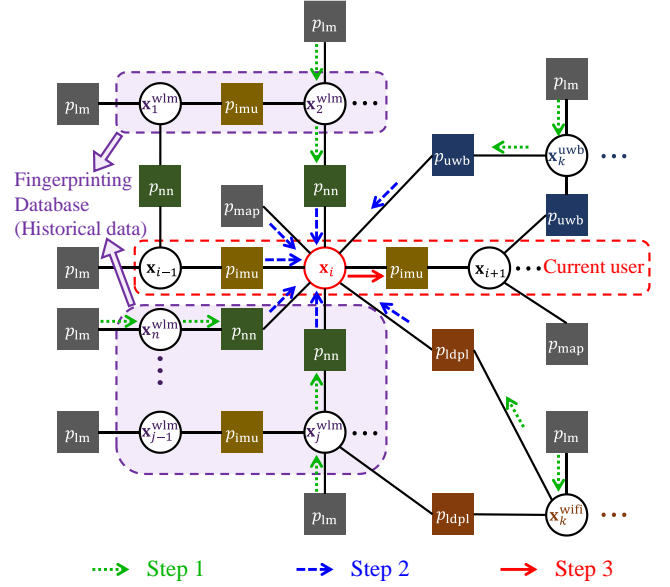
the current user node on the factor graph, while the historical data have been exploited for constructing a fingerprinting database through crowdsourcing and the related messages are no longer updated.[4] The low-complexity scheduling shown in Fig. 3 is summarized as follows:

Step 1: Calculate the messages from landmark-related *a priori* FNs to likelihood FNs according to (20) and (19) sequentially, which are represented by the green dotted arrows, for initialization.

Step 2: Calculate the messages from FNs to VNs according to (20), (22) or (23) in parallel, which are represented by the blue dashed arrows.

Step 3: Calculate the belief of $\mathbf{x}_i$ according to (19), which are represented by the red solid arrows.

In this way, we only have to conduct a single iteration for calculating a few messages during a localization process, which significantly reduces the computational complexity. Compared to the flooding scheduling, since only the backward messages related to the current user are not exploited with the aid of crowdsourcing, the performance loss is negligible.

IV. EXPERIMENTS

We built the prototype of our UWB and Wi-Fi hybrid localization system in a typical office building. The prototype is implemented by employing UWB devices, Bluetooth devices and Samsung Galaxy S7 smartphones, which have both accelerometer sensors and Wi-Fi modules. The UWB devices are integrated with the chip DW1000 of Decawave. The UWB ranging measurements are transmitted to the smartphone through the Bluetooth module HC-06. Fig. 4 illustrates the integrated client and the demo app of our localization system. The experimental region is one floor of the office building with

---

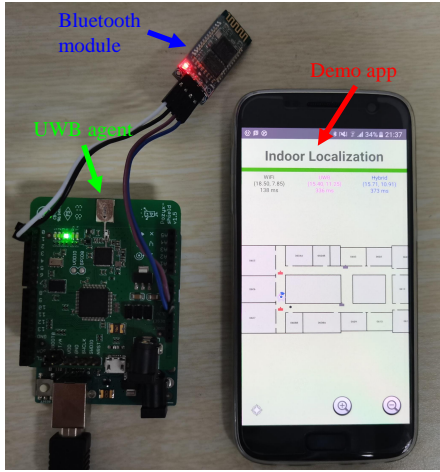[4]After crowdsourcing, the historical data can be represented by Wi-Fi landmarks.

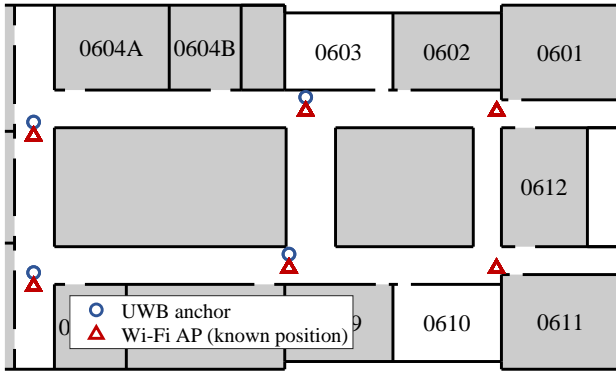Fig. 4. Integrated client and demo app of the localization system.

Fig. 5. Floor plan of the experimental region.

TABLE III
MODEL PARAMETERS

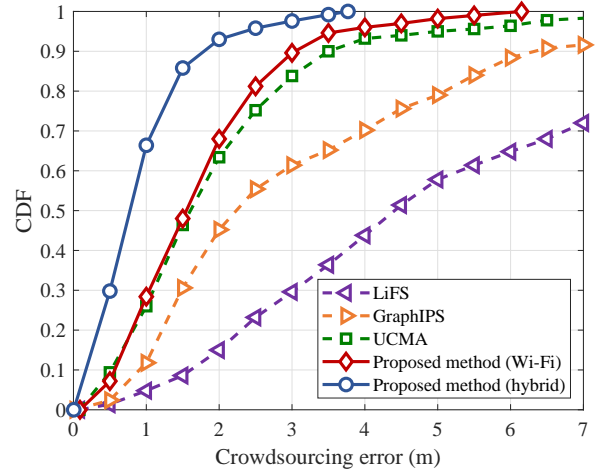| Model	Parameter	Value
UWB ranging	Noise variance σ_{u}^2	0.25
	Bias parameter ξ_{u}	2
	Maximum value $d_{\max}^{\mathrm{u}}$	40
	Outlier occurrence probability p_{o}	0.01
LDPL model	Reference distance d_0	1
	Constant β	-44
	Path loss exponent γ (LOS / NLOS)	1.85 / 3
	Variance σ_{ldpl}^2	49
Proximity model	Constant σ_{nn}	3
IMU	Variance σ_{imu}^2	0.36

Fig. 6. Performance comparison of the proposed method and the state-of-the-art methods for crowdsourcing.

a few pedestrians and obstacles, having the size of 43.9 m × 26.4 m (about 429 m²), as the white part shown in Fig. 5. More than 100 Wi-Fi APs can be detected, of which 6 have known positions, while only 4 UWB anchors are deployed.

We collect 1000 groups of test data, comprising 40 predetermined trajectories, each of which contains 25 observations, whose ground-truth positions are acquired by the labels on the ground. The observations are recorded simultaneously by the smartphone and the UWB agent every 1~3 m (about 2 s) during walking. Unless otherwise specified, 500 groups of data are applied for crowdsourcing (crowdsourcing data), and others for real-time localization (real-time data). All the data are considered to have no ground-truth position labels when used in crowdsourcing, that is, no Wi-Fi landmarks are utilized in crowdsourcing. The comparisons of all the schemes are carried out by relying on the same data as the proposed method.

The model parameters employed in the algorithms are set based on engineering experience, as summarized in Table III. In particular, the parameters of the LDPL model can be obtained by training by relying on small amounts of data or using the methods in UCMA or GraphIPS. For the proximity model, considering the environmental variations, we set σ_{nn} slightly higher than the empirical RMSE of the NN-based fingerprinting to ensure the robustness of the algorithm. The

choice of K in the proximity model depends on the data density ρ, which equals the total number of Wi-Fi landmarks plus user observations divided by the area of the accessible region. We set $K = \lceil 4\rho \rceil$, the number of iterations to $T_{\mathrm{iter}} = 5$, the grid size to $l_{\mathrm{g}} = 1$ and the number of belief samples to $N_{\mathrm{b}} = 30$, unless otherwise specified.

A. Localization Performance

We evaluate the proposed algorithm based on our unified framework in crowdsourcing and real-time localization scenarios. Both a pure Wi-Fi-based system dispensing with UWB ranging and our hybrid system are considered.

The cumulative distribution functions (CDFs) of crowdsourcing errors indicating the localization errors of crowdsourcing data recorded both for the proposed method and for the state-of-the-art algorithms are depicted in Fig. 6. Furthermore, their mean absolute errors (MAEs) and maximum errors (MaxEs) are listed in Table IV. In the LiFS method of [25], we employ the positions of the Wi-Fi APs as the key points and set the merging threshold to 100 according to

TABLE IV
CROWDSOURCING ERROR

System	Method	MAE (m)	MaxE (m)
Wi-Fi	LiFS	5.32	16.06
	GraphIPS	3.10	10.85
	UCMA	1.98	16.06
	Proposed method	1.73	6.15
Hybrid	Proposed method	0.91	3.77

TABLE V
REAL-TIME LOCALIZATION ERROR

System	Method	MAE (m)	MaxE (m)
Wi-Fi	Particle filter	4.02	43.53
	GT + WKNN	1.50	7.51
	GT + Horus	1.45	10.99
	Proposed method	1.79	6.43
	GT + proposed method	1.42	5.22
Hybrid	TSML	> 5.21	/
	Particle filter	0.97	5.01
	Proposed method	0.93	4.29
	GT + proposed method	0.84	3.77

Fig. 7. Performance comparison of the proposed method and the existing benchmark methods for real-time localization.

our experimental environments. It can be observed that, due to the naive merging of Wi-Fi fingerprints and the cumulative errors of pairwise distances encountered by the Floyd-Warshall algorithm, LiFS suffers from severe performance loss. Since the GraphIPS solution of [26] cannot accurately exploit the LDPL model without LOS information and neglects the uncertainties of different measurements, its performance also degrades significantly. For the UCMA scheme of [27], since the position proximity information provided by Wi-Fi fingerprints is not taken into consideration, the performance is adversely affected. Since the proposed method fuses heterogeneous multi-source information and exploits the uncertainties of various measurements, it outperforms the aforementioned methods in the Wi-Fi-based system and achieves sub-meter accuracy in our hybrid system.

The CDFs and the real-time localization error values are portrayed both for the proposed method and for the existing benchmark algorithms in Fig. 7 and Table V, respectively. Since our method outperforms LiFS, GraphIPS and UCMA in crowdsourcing, the real-time localization performance of these benchmark schemes is not evaluated. For the particle-filter-based solution of [31], the number of samples is set to 200 in both systems for obtaining a performance approaching the infinite-sample limit (as indicated by the curve representing the regularized importance-resampling in Fig. 12). As for Wi-Fi-based localization, since the particle filter cannot exploit the fingerprinting information, it has a poor performance. When employing the ground-truth (GT) position labels for crowdsourcing data to construct a fingerprinting database, we find that the proposed method based on serial scheduling outperforms both the weighted KNN (WKNN) algorithm and the Horus method of [34]. Indeed, our proposed method
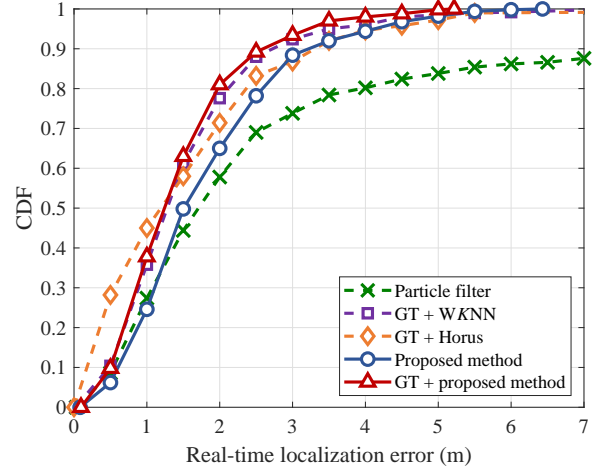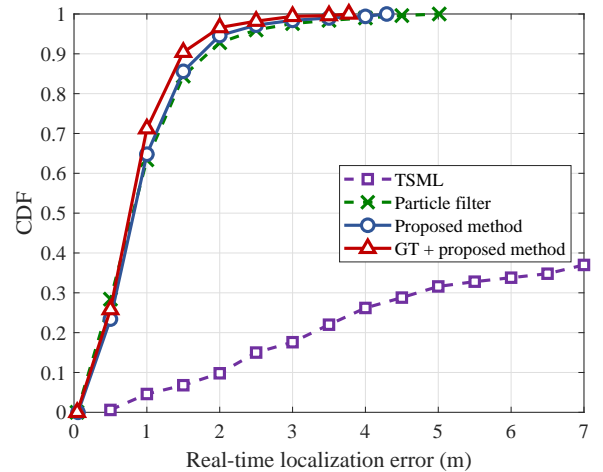
without the GT labels also achieves a comparable performance to the GT-label-aided fingerprinting. For the hybrid system, due to the scarcity of APs and the presence of obstacles, the two-stage maximum-likelihood (TSML) algorithm of [32] fails, when the number of LOS measurements is less than 3. Since the lack of fingerprinting information can be partially compensated by redundant UWB ranging, the performance of the particle filter is comparable to that of the proposed method. In fact, in our unified framework, the particle filter can be considered as a specific message passing algorithm constructed on factor graphs without loops. Furthermore, the MAE of the proposed method is less than 0.9 m with the aid of the GT labels.

B. Proximity Model

The CDFs of localization errors both with and without the proximity information (PI) provided by the proposed proximity model are shown in Fig. 8. For the Wi-Fi-based system, the proximity model is quite efficient in terms of improving the localization performance under our unified framework. For the
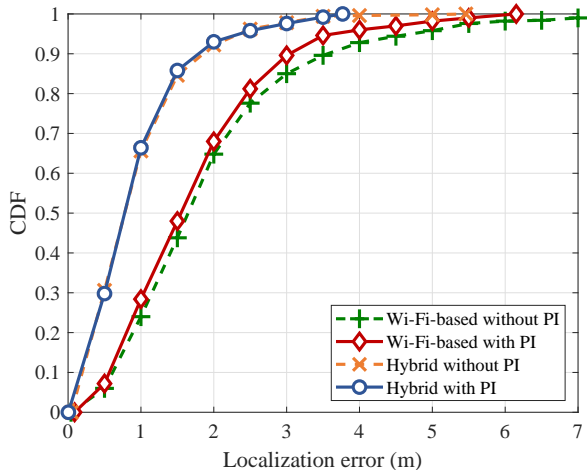
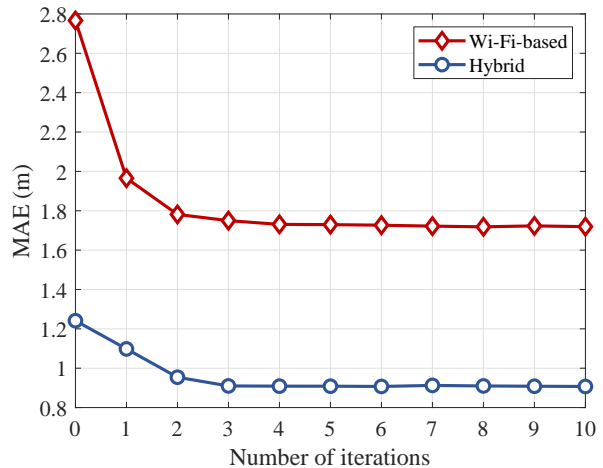Fig. 8. CDF of localization error with/without proximity information.

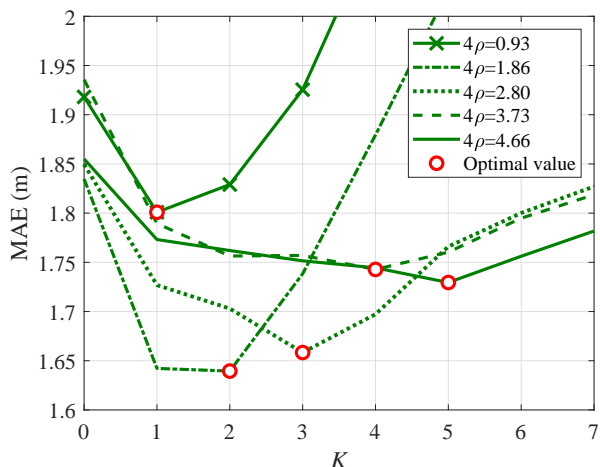Fig. 10. MAE of localization versus the number of iterations.
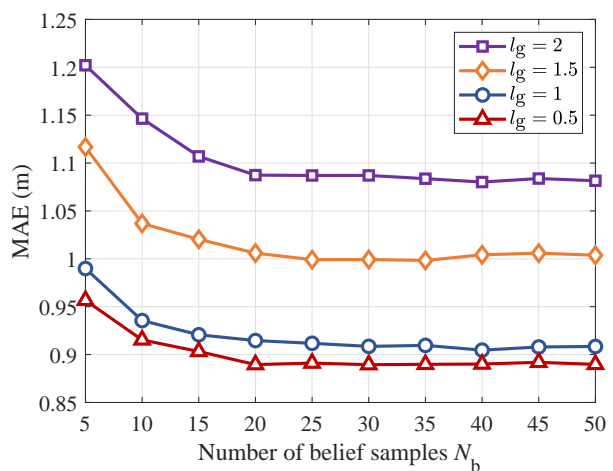

Fig. 9. MAE of localization versus the value of K.

Fig. 11. MAE of localization versus the grid size l_{g} and the number of belief samples N_{b}.

hybrid system, the proximity model is still efficient at least in terms of reducing the maximum error.

In Fig. 9, the impact of the KNN algorithm's K factor on the performance of Wi-Fi-based localization is evaluated. We utilize 100~500 groups of data to evaluate the MAE, and the corresponding data density ρ is 0.23~1.17 m^{-2}. It is observed that the optimal value of K approximately equals to $\lceil 4\rho \rceil$, which is also applicable to the hybrid system.

C. Efficiency Evaluation

The MAE of localization versus the number of iterations T_{iter} is plotted in Fig. 10. We can see that the proposed method converges within 5 iterations in both systems.

Since the sample-based scheme may lead to high computational complexity, we investigate the effects of the grid size l_{g} and the number of belief samples N_{b} on the localization performance attained by the hybrid system. In Fig. 11, it is observed that increasing l_{g} and N_{b} improves the localization performance. However, the performance gain becomes marginal beyond a certain value. Accordingly, we are able to

strike an attractive performance vs. complexity compromise by choosing the appropriate values of l_{g} and N_{b}, e.g., $l_{\mathrm{g}} = 1$ and $N_{\mathrm{b}} = 30$, resulting in $N_{\mathrm{g}} = 429$ number of grid samples.

Furthermore, in Fig. 12, we evaluate the localization performance versus the computational complexity for the grid sampling method of [47], for the regularized importance-resampling [48] and for the proposed sampling method. The complexity of the proposed method is on the order of $\mathcal{O}\left[(N_{\mathrm{b}} + N_{\mathrm{g}}) N_{\mathrm{b}}\right]$, while that of the other two schemes is on the order of $\mathcal{O}\left(N_{\mathrm{s}}^2\right)$, where N_{s} is the number of samples. Since the grid size l_{g} significantly affects the performance as shown in Fig. 11, we also evaluate the proposed scheme using different l_{g} values in Fig. 12. It is observed that the proposed method outperforms both the grid sampling and the regularized importance-resampling schemes at a lower complexity, when $l_{\mathrm{g}} \leqslant 1$. Additionally, for $l_{\mathrm{g}} = 1$, we can achieve a comparable performance to $l_{\mathrm{g}} = 0.5$ at a lower complexity, which is much preferred in the scenario considered.
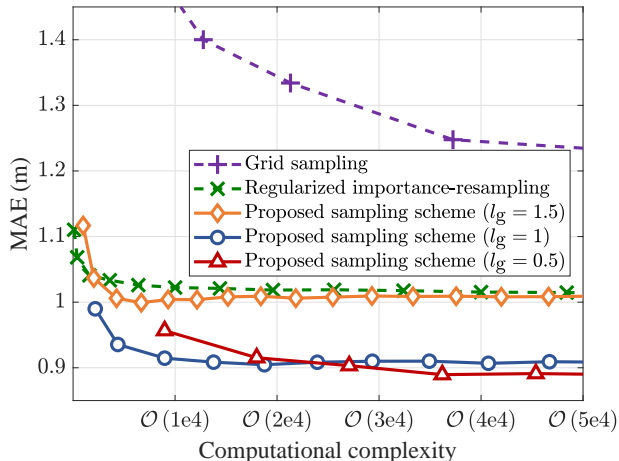
Fig. 12. MAE of localization versus the computational complexity.

TABLE VI
LOCALIZATION ERRORS OF VARIOUS MEASUREMENT COMBINATIONS

	MAE (m)	MaxE (m)
UWB only	4.53	34.06
UWB + IMU	1.24	11.49
Wi-Fi only	2.39	9.07
Wi-Fi + IMU	1.73	6.15
UWB + Wi-Fi	1.00	5.50
All	0.91	3.77

(a) UWB only (b) UWB + IMU

(c) Wi-Fi only (d) Wi-Fi + IMU

(e) UWB + Wi-Fi (f) All

Fig. 13. Heatmap of localization error for various combinations of measurements.

TABLE VII
LOCALIZATION PERFORMANCE WITH/WITHOUT OUTLIER DETECTION

	MAE (m)	MaxE (m)
Without OD	1.05	22.09
With OD	0.91	3.77

D. Information Fusion

Based on our hybrid system, we now investigate the localization performance of the proposed method for various combinations of measurements via heatmaps, as shown in Fig. 13. Their MAEs and maximum errors are listed in Table VI. Due to the scarcity of UWB anchors, there are many localization blind spots when only UWB ranging measurements are exploited. By contrast, Wi-Fi fingerprints can provide ubiquitous localization, but at a relatively low accuracy. By integrating the IMU measurements, the accuracy of both UWB-based and Wi-Fi-based localization is significantly improved. Moreover, the fusion of UWB ranging and Wi-Fi fingerprinting can effectively eliminate the localization blind spots, thus further improving the overall performance. Fusing all the measurements based on the proposed algorithm is able to provide the best performance. The result indicates that the proposed framework succeeds in efficiently fusing the multi-source information in various types of measurements to achieve ubiquitous high-accuracy indoor localization.

E. Outlier Detection

Let us now evaluate the proposed outlier detection (OD) approach in our hybrid system. Table VII shows the localization performance both with and without outlier detection. It is observed that the proposed outlier detector significantly reduces the maximum localization error, which will create an improved user experience.
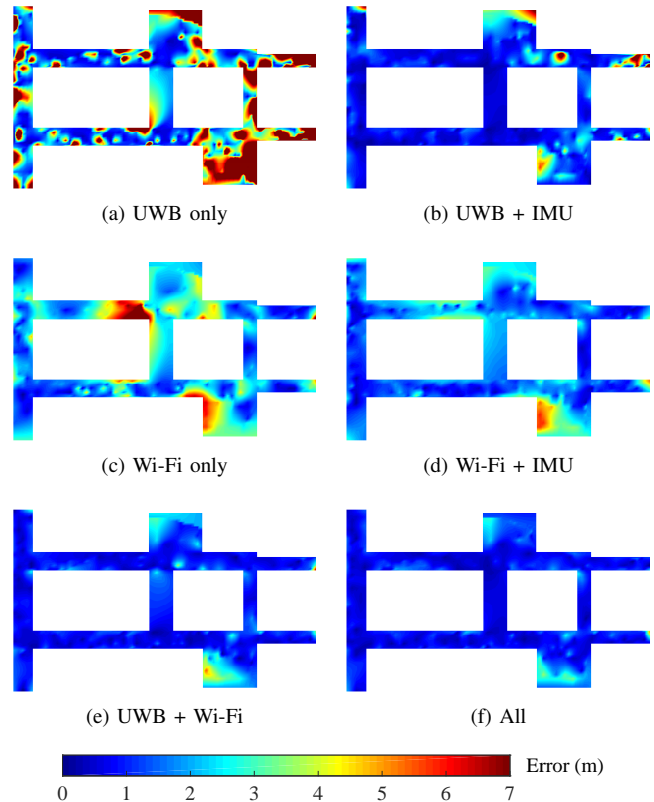
F. Serial Scheduling

We investigate the performance loss of serial scheduling relying on the crowdsourcing database compared to the flooding-based scheduling, as shown in Fig. 14. Observe that the performance loss of the serial scheduling scheme is negligible in both systems, which also demonstrates that the crowdsourcing succeeds in sufficiently squeezing the information contained in the historical data and facilitates real-time localization by relying on the database constructed. The only reason for the performance loss of the serial scheduling is the lack of backward tracing and cooperation.

G. Long-Term Evaluation

To evaluate the user experience of the proposed localization method, we characterize its long-term operation by exploiting all the test data. Assume that an observation is obtained every 2 s, and the Wi-Fi fingerprinting database is updated every 50 s based on the existing observations. The real-time localization errors of the proposed method are shown in Fig. 15. The solid curves depict the MAEs during the past 50 s and the
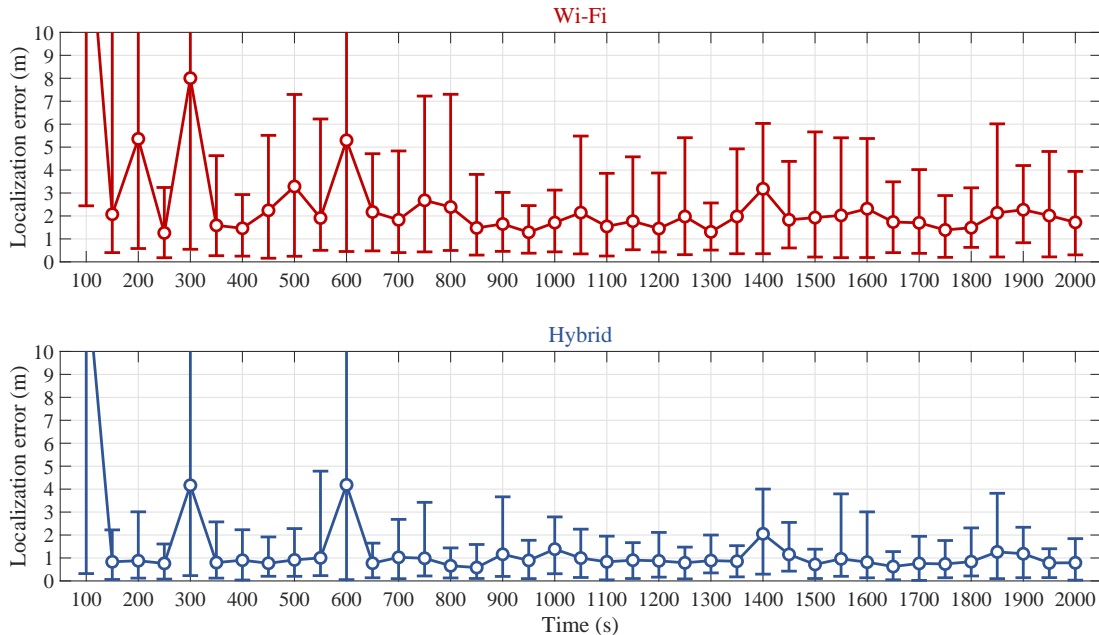
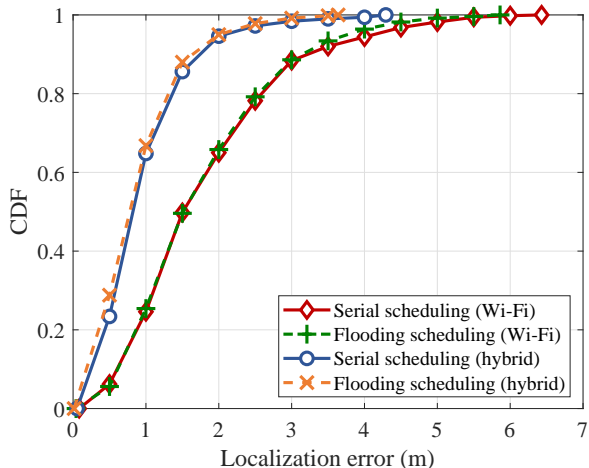Fig. 15. Real-time localization error during long-term use.

Fig. 14. CDF of localization error using different scheduling.

uitous indoor localization. In this contribution, we proposed a unified framework for ranging-based and fingerprint-aided localization relying on factor graphs and developed a non-parametric BP algorithm for estimating the positions. Furthermore, we proposed an outlier detection technique based on the likelihood ratio. For designing real-time localization, we conceived serial message scheduling for reducing the computational complexity imposed. The experiments conducted by harnessing our hybrid UWB and Wi-Fi localization system show that the proposed method outperforms the existing state-of-the-art methods and achieves sub-meter-level localization accuracy without excessive infrastructure investment and costly site surveys. This work provides a spring-board for diverse indoor localization applications.

vertical intervals represent the maximum and minimum values determined by the error bars. It is seen that upon increasing the service time, both accuracy and robustness of both localization systems can be improved. After 800 s, the MAE for the Wi-Fi-based and for our hybrid system remains around 2 m and 1 m, respectively, while the maximum error is less than 6 m and 4 m. This long-term evaluation confirms that the proposed unified framework efficiently exploits the incremental data to facilitate real-time localization, and hence improves the user experience in practical applications.

V. CONCLUSIONS

Integrating ranging and fingerprinting with crowdsourcing constitutes a promising techniques of achieving accurate ubiq-

REFERENCES

[1] Y. Fu, P. Chen, S. Yang, and J. Tang, "An indoor localization algorithm based on continuous feature scaling and outlier deleting," *IEEE Internet Things J.*, vol. 5, no. 2, pp. 1108–1115, Apr. 2018.

[2] Y. Zhou, L. Liu, L. Wang, N. Hui, X. Cui, J. Wu, Y. Peng, Y. Qi, and C. Xing, "Service-aware 6G: An intelligent and open network based on the convergence of communication, computing and caching," *Digit. Commun. Netw.*, vol. 6, no. 3, pp. 253–260, Aug. 2020.

[3] Y. Zhou, H. Liu, Z. Pan, L. Tian, and J. Shi, "Cooperative multicast with location aware distributed mobile relay selection: Performance analysis and optimized design," *IEEE Trans. Veh. Technol.*, vol. 66, no. 9, pp. 8291–8302, Sep. 2017.

[4] P. S. Farahsari, A. Farahzadi, J. Rezazadeh, and A. Bagheri, "A survey on indoor positioning systems for IoT-based applications," *IEEE Internet Things J.*, vol. 9, no. 10, pp. 7680–7699, May 2022.

[5] R. S. Shit, S. Sharma, D. Puthal, and A. Y. Zomaya, "Location of things (LoT): A review and taxonomy of sensors localization in IoT infrastructure," *IEEE Commun. Surveys Tuts.*, vol. 20, no. 3, pp. 2028–2061, 3rd Quart. 2018.

[6] S. He and S.-H. G. Chan, "Wi-Fi fingerprint-based indoor positioning: Recent advances and comparisons," *IEEE Commun. Surveys Tuts.*, vol. 18, no. 1, pp. 466–490, 1st Quart. 2016.

[7] W. Li, C. Zhang, and Y. Tanaka, "Pseudo label-driven federated learning-based decentralized indoor localization via mobile crowdsourcing," *IEEE Sensors J.*, vol. 20, no. 19, pp. 11 556–11 565, Oct. 2020.

[8] A. Yassin, Y. Nasser, M. Awad, A. Al-Dubai, R. Liu, C. Yuen, R. Raulefs, and E. Aboutanios, "Recent advances in indoor localization: A survey on theoretical approaches and applications," *IEEE Commun. Surveys Tuts.*, vol. 19, no. 2, pp. 1327–1346, 2nd Quart. 2017.

[9] Y. Xu, Y. S. Shmaliy, Y. Li, X. Chen, and H. Guo, "Indoor INS/LiDAR-based robot localization with improved robustness using cascaded FIR filter," *IEEE Access*, vol. 7, pp. 34 189–34 197, 2019.

[10] Y. Xu, Y. S. Shmaliy, Y. Li, and X. Chen, "UWB-based indoor human localization with time-delayed data using EFIR filtering," *IEEE Access*, vol. 5, pp. 16 676–16 683, 2017.

[11] Y. Yu, R. Chen, L. Chen, X. Zheng, D. Wu, W. Li, and Y. Wu, "A novel 3-D indoor localization algorithm based on BLE and multiple sensors," *IEEE Internet Things J.*, vol. 8, no. 11, pp. 9359–9372, Jun. 2021.

[12] J. Niu, B. Wang, L. Shu, T. Q. Duong, and Y. Chen, "ZIL: An energy-efficient indoor localization system using ZigBee radio to detect WiFi fingerprints," *IEEE J. Sel. Areas Commun.*, vol. 33, no. 7, pp. 1431–1442, Jul. 2015.

[13] P. Bahl and V. N. Padmanabhan, "RADAR: An in-building RF-based user location and tracking system," in *Proc. IEEE INFOCOM*, vol. 2, Tel Aviv, Israel, Mar. 2000, pp. 775–784.

[14] Y. Zheng, M. Sheng, J. Liu, and J. Li, "Exploiting AoA estimation accuracy for indoor localization: A weighted AoA-based approach," *IEEE Wireless Commun. Lett.*, vol. 8, no. 1, pp. 65–68, Feb. 2019.

[15] A. Alteneiji, U. Ahmad, K. Poon, N. Ali, and N. Almoosa, "Indoor localization in multi-path environment based on AoA with particle filter," in *Proc. IEEE ICSPIS*, Dubai, UAE, Nov. 2020, pp. 1–4.

[16] L. Chen, K. Yang, and X. Wang, "Robust cooperative Wi-Fi fingerprint-based indoor localization," *IEEE Internet Things J.*, vol. 3, no. 6, pp. 1406–1417, Dec. 2016.

[17] J. Luo, Z. Zhang, C. Liu, and H. Luo, "Reliable and cooperative target tracking based on WSN and WiFi in indoor wireless networks," *IEEE Access*, vol. 6, pp. 24 846–24 855, 2018.

[18] S. Wang, F. Luo, and L. Zhang, "Universal cooperative localizer for WSN with varied types of ranging measurements," *IEEE Signal Process. Lett.*, vol. 24, no. 8, pp. 1223–1227, Aug. 2017.

[19] I. Guvenc and C. Chong, "A survey on TOA based wireless localization and nlos mitigation techniques," *IEEE Communications Surveys Tutorials*, vol. 11, no. 3, pp. 107–124, 3rd Quart. 2009.

[20] K. C. Ho, "Bias reduction for an explicit solution of source localization using TDOA," *IEEE Trans. Signal Process.*, vol. 60, no. 5, pp. 2101–2114, May 2012.

[21] K. N. R. S. V. Prasad and V. K. Bhargava, "RSS localization under Gaussian distributed path loss exponent model," *IEEE Wireless Commun. Lett.*, vol. 10, no. 1, pp. 111–115, Jan. 2021.

[22] X. Wang, L. Gao, S. Mao, and S. Pandey, "CSI-based fingerprinting for indoor localization: A deep learning approach," *IEEE Trans. Veh. Technol.*, vol. 66, no. 1, pp. 763–776, Jan. 2017.

[23] B. Ferris, D. Fox, and N. D. Lawrence, "WiFi-SLAM using Gaussian process latent variable models," in *Proc. IJCAI*, Hyderabad, India, Jan. 2007, pp. 2480–2485.

[24] X. Wang, X. Wang, S. Mao, J. Zhang, S. C. G. Periaswamy, and J. Patton, "Indoor radio map construction and localization with deep Gaussian processes," *IEEE Internet Things J.*, vol. 7, no. 11, pp. 11 238–11 249, Nov. 2020.

[25] C. Wu, Z. Yang, and Y. Liu, "Smartphones based crowdsourcing for indoor localization," *IEEE Trans. Mobile Comput.*, vol. 14, no. 2, pp. 444–457, Feb. 2015.

[26] Y. Zhao, Z. Zhang, T. Feng, W. C. Wong, and H. K. Garg, "GraphIPS: Calibration-free and map-free indoor positioning using smartphone crowdsourced data," *IEEE Internet Things J.*, vol. 8, no. 1, pp. 393–406, Jan. 2021.

[27] S. Jung, B. Moon, and D. Han, "Unsupervised learning for crowdsourced indoor localization in wireless networks," *IEEE Trans. Mobile Comput.*, vol. 15, no. 11, pp. 2892–2906, Nov. 2016.

[28] A. Rai, K. K. Chintalapudi, V. N. Padmanabhan, and R. Sen, "Zee: Zero-effort crowdsourcing for indoor localization," in *Proc. ACM MobiCom*, Istanbul, Turkey, Aug. 2012, pp. 293–304.

[29] G. Huang, Z. Hu, J. Wu, H. Xiao, and F. Zhang, "WiFi and vision-integrated fingerprint for smartphone-based self-localization in public indoor scenes," *IEEE Internet Things J.*, vol. 7, no. 8, pp. 6748–6761, Aug. 2020.

[30] Y. Zhao, J. Xu, J. Wu, J. Hao, and H. Qian, "Enhancing camera-based multimodal indoor localization with device-free movement measurement using WiFi," *IEEE Internet Things J.*, vol. 7, no. 2, pp. 1024–1038, Feb. 2020.

[31] N. Bargshady, K. Pahlavan, and N. A. Alsindi, "Hybrid WiFi/UWB, cooperative localization using particle filter," in *Proc. IEEE ICNC*, Garden Grove, California, USA, Feb. 2015, pp. 1055–1060.

[32] S. Monica and F. Bergenti, "Hybrid indoor localization using WiFi and UWB technologies," *Electron.*, vol. 8, no. 3, p. 334, Mar. 2019.

[33] J.-H. Seong, E.-C. Choi, J.-S. Lee, and D.-H. Seo, "High-speed positioning and automatic updating technique using Wi-Fi and UWB in a ship," *Wireless Pers. Commun.*, vol. 94, no. 3, pp. 1105–1121, Jun. 2017.

[34] M. Youssef and A. K. Agrawala, "The Horus WLAN location determination system," in *Proc. ACM MobiSys*, Seattle, Washington, USA, Jun. 2005, pp. 205–218.

[35] B. Lashkari, J. Rezazadeh, R. Farahbakhsh, and K. Sandrasegaran, "Crowdsourcing and sensing for indoor localization in IoT: A review," *IEEE Sensors J.*, vol. 19, no. 7, pp. 2408–2434, Apr. 2019.

[36] B. Jang and H. Kim, "Indoor positioning technologies without offline fingerprinting map: A survey," *IEEE Commun. Surveys Tuts.*, vol. 21, no. 1, pp. 508–525, 1st Quart. 2019.

[37] X. Guo, N. Ansari, F. Hu, Y. Shao, N. R. Elikplim, and L. Li, "A survey on fusion-based indoor positioning," *IEEE Commun. Surveys Tuts.*, vol. 22, no. 1, pp. 566–594, 1st Quart. 2020.

[38] R. Harle, "A survey of indoor inertial positioning systems for pedestrians," *IEEE Commun. Surveys Tuts.*, vol. 15, no. 3, pp. 1281–1293, 3rd Quart. 2013.

[39] H.-A. Loeliger, "An introduction to factor graphs," *IEEE Signal Process. Mag.*, vol. 21, no. 1, pp. 28–41, Jan. 2004.

[40] H. Wymeersch, J. Lien, and M. Z. Win, "Cooperative localization in wireless networks," *Proc. IEEE*, vol. 97, no. 2, pp. 427–450, Feb. 2009.

[41] W. Yuan, N. Wu, Q. Guo, X. Huang, Y. Li, and L. Hanzo, "TOA-based passive localization constructed over factor graphs: A unified framework," *IEEE Trans. Commun.*, vol. 67, no. 10, pp. 6952–6965, Oct. 2019.

[42] C. Xu, Y. Shi, J. Wan, and S. Duan, "Uncertainty constrained belief propagation for cooperative target tracking," *IEEE Internet Things J.*, vol. 9, no. 19, pp. 19 414–19 425, Oct. 2022.

[43] J. Xu, G. Yang, Y. Sun, and S. Picek, "A multi-sensor information fusion method based on factor graph for integrated navigation system," *IEEE Access*, vol. 9, pp. 12 044–12 054, 2021.

[44] W. Zhao, W. Meng, Y. Chi, and S. Han, "Factor graph based multi-source data fusion for wireless localization," in *Proc. IEEE WCNC*, Doha, Qatar, Apr. 2016, pp. 1–6.

[45] K. Chintalapudi, A. P. Iyer, and V. N. Padmanabhan, "Indoor localization without the pain," in *Proc. ACM MobiCom*, Chicago, Illinois, USA, Sep. 2010, pp. 173–184.

[46] Y. Xiong, N. Wu, H. Wang, and J. Kuang, "Cooperative detection-assisted localization in wireless networks in the presence of ranging outliers," *IEEE Trans. Commun.*, vol. 65, no. 12, pp. 5165–5179, Dec. 2017.

[47] M. Nicoli, C. Morelli, and V. Rampa, "A jump Markov particle filter for localization of moving terminals in multipath indoor scenarios," *IEEE Trans. Signal Process.*, vol. 56, no. 8, pp. 3801–3809, Aug. 2008.

[48] M. S. Arulampalam, S. Maskell, N. Gordon, and T. Clapp, "A tutorial on particle filters for online nonlinear/non-Gaussian Bayesian tracking," *IEEE Trans. Signal Process.*, vol. 50, no. 2, pp. 174–188, Feb. 2002.

[49] R. Mendrzik and G. Bauch, "Position-constrained stochastic inference for cooperative indoor localization," *IEEE Trans. Signal Inf. Process. Netw.*, vol. 5, no. 3, pp. 454–468, Sep. 2019.

[50] W. Sun, J. Liu, C. Wu, Z. Yang, X. Zhang, and Y. Liu, "MoLoc: On distinguishing fingerprint twins," in *Proc. IEEE ICDCS*, Philadelphia, Pennsylvania, USA, Jul. 2013, pp. 226–235.

[51] J.-H. Jun, Y. Gu, L. Cheng, B. Lu, J. Sun, T. Zhu, and J. Niu, "Social-Loc: Improving indoor localization with social sensing," in *Proc. ACM SenSys*, Roma, Italy, Nov. 2013, pp. 14:1–14:14.

[52] J. Y. Zhu, A. X. Zheng, J. Xu, and V. O. K. Li, "Spatio-temporal (S-T) similarity model for constructing WIFI-based RSSI fingerprinting map for indoor localization," in *Proc. IEEE IPIN*, Busan, Korea (South), Oct. 2014, pp. 678–684.

[53] N. Saccomanno, A. Brunello, and A. Montanari, "What you sense is not where you are: On the relationships between fingerprints and spatial knowledge in indoor positioning," *IEEE Sensors J.*, vol. 22, no. 6, pp. 4951–4961, Mar. 2022.

[54] Q. Chen and B. Wang, "FinCCM: Fingerprint crowdsourcing, clustering and matching for indoor subarea localization," *IEEE Wireless Commun. Lett.*, vol. 4, no. 6, pp. 677–680, Dec. 2015.

[55] M. Luo, J. Zheng, W. Sun, and X. Zhang, "WiFi-based indoor localization using clustering and fusion fingerprint," in *Proc. IEEE CCC*, Shanghai, China, Jul. 2021, pp. 3480–3485.

[56] Z. Yang, X. Feng, and Q. Zhang, "Adometer: Push the limit of pedestrian indoor localization through cooperation," *IEEE Trans. Mobile Comput.*, vol. 13, no. 11, pp. 2473–2483, Nov. 2014.

[57] F. R. Kschischang and B. J. Frey, "Iterative decoding of compound codes by probability propagation in graphical models," *IEEE J. Sel. Areas Commun.*, vol. 16, no. 2, pp. 219–230, Feb. 1998.

[58] H. Wang, H. Li, J. Fang, and H. Wang, "Robust Gaussian Kalman filter with outlier detection," *IEEE Signal Process. Lett.*, vol. 25, no. 8, pp. 1236–1240, Aug. 2018.

Lyuxiao Yang (Student Member, IEEE) received the B.S. degree in electronic engineering from Beijing Institute of Technology (BIT), Beijing, China, in 2017. He is currently working toward the Ph.D. degree with the School of Information and Electronics, BIT. His research interests include indoor localization, cooperative localization, and statistical inference on graphical models.

Nan Wu (Member, IEEE) received the B.S., M.S., and Ph.D. degrees from Beijing Institute of Technology (BIT), Beijing, China, in 2003, 2005, and 2011, respectively. From 2008 to 2009, he was a Visiting Ph.D. Student with the Department of Electrical Engineering, Pennsylvania State University, USA. He is currently a Professor with the School of Information and Electronics, BIT. His research interests include signal processing in wireless communication networks. He was a recipient of the National Excellent Doctoral Dissertation Award by MOE of China in 2013. He serves as an Editorial Board Member for the *IEEE Wireless Communications Letters*.

Bin Li (Member, IEEE) received the B.S. degree in information engineering and the M.S. degree in information and communication engineering from Beijing Institute of Technology (BIT), Beijing, China, in 2012 and 2015, respectively, and the Ph.D. degree in electrical and electronic engineering from the University of Hong Kong, Hong Kong, in 2019. He is currently an Assistant Professor with the School of Information and Electronics, BIT. His research interests include signal processing, wireless communications, and machine learning. He serves as an Editorial Board Member of *IEICE Transactions on Communications* and *KSII Transactions on Internet and Information Systems*.

Weijie Yuan (Member, IEEE) received the B.S. degree from the Beijing Institute of Technology, China, in 2013, and the Ph.D. degree from the University of Technology Sydney, Australia, in 2019. In 2016, he was a Visiting Ph.D. Student with the Institute of Telecommunications, Vienna University of Technology, Austria. He was a Research Assistant with the University of Sydney, a Visiting Associate Fellow with the University of Wollongong, and a Visiting Fellow with the University of Southampton, from 2017 to 2019. From 2019 to 2021, he was a Research Associate with the University of New South Wales. He is currently an Assistant Professor with the Department of Electrical and Electronic Engineering, Southern University of Science and Technology, Shenzhen, China. He was a recipient of the Best Ph.D. Thesis Award from the Chinese Institute of Electronics and an Exemplary Reviewer from IEEE TCOM/WCL. He currently serves as an Associate Editor for the *IEEE Communications Letters*, an Associate Editor and an Award Committee Member for the *EURASIP Journal on Advances in Signal Processing*. He has led the guest editorial teams for three special issues in *IEEE Communications Magazine*, *IEEE Transactions on Green Communications and Networking*, and *China Communications*. He was an Organizer/the Chair of several workshops and special sessions on orthogonal time frequency space (OTFS) and integrated sensing and communication (ISAC) in flagship IEEE and ACM conferences, including IEEE ICC, IEEE/CIC ICCC, IEEE SPAWC, IEEE VTC, IEEE WCNC, IEEE ICASSP, and ACM MobiCom. He is the Founding Chair of the IEEE ComSoc Special Interest Group on Orthogonal Time Frequency Space (OTFS-SIG).

Lajos Hanzo (Life Fellow, IEEE) received his Master degree and Doctorate in 1976 and 1983, respectively from the Technical University (TU) of Budapest. He was also awarded the Doctor of Sciences (DSc) degree by the University of Southampton (2004) and Honorary Doctorates by the TU of Budapest (2009) and by the University of Edinburgh (2015). He is a Foreign Member of the Hungarian Academy of Sciences and a former Editor-in-Chief of the IEEE Press. He has served several terms as Governor of both IEEE ComSoc and of VTS. He has published 2000+ contributions at IEEE Xplore, 19 Wiley-IEEE Press books and has helped the fast-track career of 123 PhD students. Over 40 of them are Professors at various stages of their careers in academia and many of them are leading scientists in the wireless industry. He is also a Fellow of the Royal Academy of Engineering (FREng), of the IET and of EURASIP. He holds the Eric Sumner Field Award. (http://www-mobile.ecs.soton.ac.uk, https://en.wikipedia.org/wiki/Lajos_Hanzo)